The Astrophysical Journal Supplement Series, 157:396–401, 2005 April

PLASMA AND MAGNETIC FIELD PARAMETERS IN THE VICINITY OF SHORT-PERIODIC GIANT EXOPLANETS

N. V. Erkaev
Institute for Computational Modelling, Russian Academy of Sciences, 660036 Krasnoyarsk 36, Russia; erkaev@icm.krasn.ru
T. Penz,[1] H. Lammer, H. I. M. Lichtenegger, and H. K. Biernat[1,2]
Space Research Institute, Austrian Academy of Sciences, Schmiedlstrasse 6, A-8042 Graz, Austria;
thomas.penz@oeaw.ac.at.at, helmut.lammer@oeaw.ac.at
P. Wurz
Physikalisches Institut, University of Bern, Sidlerstrasse 5, CH-3012 Bern, Switzerland; peter.wurz@soho.unibe.ch
J.-M. Grießmeier
Institut für Theoretische Physik, Technische Universität Braunschweig, Mendelssohnstrasse 3, D-38106 Braunschweig, Germany;
j-m.griessmeier@tu-bs.de
and
W. W. Weiss
Department for Astronomy, University of Vienna, Türkenschanzstrasse 17, A-1180 Vienna, Austria; weiss@astro.univie.ac.at
Received 2004 July 26; accepted 2004 December 6

ABSTRACT

During the past years, more than 130 giant planets were discovered in extrasolar planetary systems. Because of the fact that the orbital distances are very close to their host stars, these planets are embedded in a dense stellar wind, which can pick up planetary ions. We model the stellar wind interaction of the short-periodic exoplanets OGLE-TR-56b and HD 209458b at their orbital distances of $\approx$0.023 AU and $\approx$0.045 AU, by calculating the Alfvén Mach number and the magnetosonic Mach number in the stellar wind plasma flow. We then analyze the different plasma interaction regimes around the planetary obstacles, which appear for different stellar wind parameters. Our study shows that the stellar wind plasma parameters like temperature, interplanetary magnetic field, particle density, and velocity near planetary obstacles at orbital distances closer than 0.1–0.2 AU have conditions such that no bow shocks evolve. Our study shows also that these close-in exoplanets are in a submagnetosonic regime comparable to the magnetospheric plasma interaction of the inner satellites of Jupiter and Saturn. Furthermore, we compare the results achieved for both exoplanets with the Jupiter-class exoplanet HD 28185b at its orbital distance of $\approx$1.03 AU. Finally, we also discuss the behavior of the stellar wind plasma flow close to the planetary obstacles of two highly eccentric gas giants, namely, HD 108147b and HD 162020b. Because of their eccentric orbits, these two exoplanets periodically experience both regimes with and without a bow shock. Finally, we simulate the neutral gas density of HD 209458b with a Monte Carlo model. By using the plasma parameters obtained in our study we calculate the ion production and loss rate of H^+ with a test particle model. Our simulations yield H^+ loss rates for HD 209458b or similar giant exoplanets in orders of about 10^8–10^9 g s^{-1}. These ion loss rates are at least 1 order of magnitude lower than the observed loss rate of evaporating neutral H atoms. Our study indicates, that similar gas giants at larger orbital distances have lower ion loss rates. Thus, the dominating component of particle loss of short-periodic Jupiter-class exoplanets will be neutral hydrogen.

Subject headings: magnetic fields — planetary systems — plasmas — shock waves — stars: winds, outflows

1. INTRODUCTION

The number of the presently discovered 130 giant exoplanets[3] will be dramatically enhanced after the launch of the CoRoT space observatory in 2006, which will use high precise photometry for planetary detection by the transit method. Within a stellar field of 3°.9 square, CoRoT will monitor simultaneously up to 12,000 stars, within a magnitude range of roughly $V = 11.5$–16, during five time slots of 150 days. By applying the statistics of discovered short periodic Jupiter-class exoplanets to the suggested 1.8×10^5 light curves obtained by CoRoT, one may expect the discovery of about 200 hot giant exoplanets ($\geq$0.1 $M_{\rm Jup}$ with orbital periods of less than 10 days) after dropping 50% of the target stars because of their radius or binarity (Moutou et al. 2003).

At present about 20% of the known exoplanets have orbital distances of less than 0.1 AU or orbital periods of less than 11 days. Recently, Vidal-Madjar et al. (2003) observed with the *Hubble Space Telescope* Imaging Spectrograph an extended and evaporating upper atmosphere around HD 209458b. A neutral hydrogen mass-loss rate $\geq 10^{10}$ g s^{-1} has been derived from the observed absorption in the Lyα emission profile. Recent observations also detected atomic oxygen and carbon beyond the Roche lobe of HD 209458b, indicating that these heavy species must be carried out up to this distance and beyond most likely in a state of hydrodynamic "blow-off" (Lammer et al. 2003; Vidal-Madjar et al. 2003, 2004; Lecavelier des Etangs et al. 2004; Baraffe et al. 2004).

[1] also at: Institute of Physics, Division for Theoretical Physics, University of Graz, Universitätsplatz 5, A-8010 Graz, Austria.
[2] also at: Institute for Geophysics, Astrophysics, and Meteorology, University of Graz, Universitätsplatz 5, A-8010 Graz, Austria.
[3] See http://www.obspm.fr/encycl/encycl.html.

Recent detailed aeronomical calculations by Yelle (2004) of the atmospheric structure of giant exoplanets in orbits with semimajor axes from 0.01–0.1 AU are in agreement with the study by Lammer et al. (2003) that the thermospheres of these hydrogen-rich gas giants can be heated to over 10,000 K by the X-ray and extreme ultraviolet (XUV) flux from the central star. These high temperatures cause the neutral atmosphere to escape rapidly, implying that the upper thermosphere is cooled primarily by adiabatic expansion. If an upper atmosphere of a planet is in full energy-limited hydrodynamic "blow-off" conditions the expansion will lead to cooler temperatures (Watson et al. 1981). The lower thermosphere is cooled primarily by radiative emissions from H_3^+, created by photoionization of H_2 and subsequent ion chemistry (Yelle 2004).

The growing evidence that these short-periodic exoplanets experience a hydrodynamic-driven atmospheric "blow-off" (Lammer et al. 2003; Vidal-Madjar et al. 2003, 2004; Lecavelier des Etangs et al. 2004; Baraffe et al. 2004) led one to consider that their extended upper atmospheres may directly interact with the incoming stellar wind plasma flow. The stellar wind plasma interaction of short-periodic exoplanets and the high XUV flux at close orbital distances play a crucial role with regard to ionization and ion loss processes of atmospheric species. These processes depend strongly on the plasma interaction regime with the planetary obstacle, which is determined by the stellar wind parameters, like the magnetosonic and Alfvén Mach numbers (Penz et al. 2004a). For magnetosonic Mach numbers greater than 1, the stellar wind interaction with a planetary obstacle results in the appearance of a bow shock separating the shocked, thermalized stellar wind plasma from the undisturbed one. If the upstream magnetosonic Mach number decreases, the bow shock becomes weaker and finally disappears when the Mach number reaches values less than 1. In such a case the stellar wind plasma flow around the planetary obstacle is not so much compressed and its temperature is not as high as in the case of a shock.

Besides the magnetosonic Mach number, the Alfvén Mach number is a key parameter for the formation of a so-called magnetic barrier, which is a layer of an enhanced magnetic field ahead of the planetary obstacle. The magnetic barrier region is the result of a stretching of the "frozen-in" interplanetary magnetic field by the stellar wind flowing around the planetary obstacle. This magnetic barrier plays an important role for the processes of mass, momentum, and energy transfer into the ionosphere of a non- or weakly magnetized planet (Erkaev et al. 2003). In particular, the magnetic barrier is a background for plasma instabilities occurring at the ionized boundary of a planetary obstacle (Arshukova et al. 2004; Penz et al. 2004b). The thickness of the magnetic barrier is in the order of the curvature radius of the obstacle to the Alfvén Mach number squared.

Grießmeier et al. (2004) modeled the stellar wind interaction of short periodic gas giants for present and for early evolutionary stages of solar-like stars and found that it may be possible that short periodic gas giants can have an ionosphere–stellar wind interaction like Venus, because the internal magnetic moment of exoplanets orbiting close to their host stars may be very weak owing to tidal locking. It was shown that the magnetic moments can be less than one tenth of the value presently observed for Jupiter at 5 AU. In such a case, the unprotected or weak protected expanded upper atmosphere will be affected by ionization and nonthermal ion loss processes, which contribute to the calculated neutral H atom mass-loss rates calculated in the orders of $\approx 10^{10}$–10^{12} g s^{-1} (Lammer et al. 2003; Lecavelier des Etangs et al. 2004; Baraffe et al. 2004). A knowledge of the loss rates of the ionized component is important, because the planetary ions may interact with magnetic flux tubes in the star-exoplanet environment comparable to an Io-Jupiter–type electrodynamic plasma interaction (Zarka et al. 2001), or they may be accelerated by magnetic reconnection and directed to the host stars surface, where chromospheric heating and flarelike processes could be triggered (Ip et al. 2004; Rubenstein & Schäfer 2000; Cuntz et al. 2000; Cuntz & Shkolnik 2002).

The aim of this work is to calculate planetary ion loss rates by analyzing the behavior of the magnetosonic and Alfvén Mach numbers in the plasma environment of close-in gas giants like OGLE-TR-56b (Konacki et al. 2003; Burrows et al. 2004) and HD 209458b (Lammer et al. 2003; Vidal-Madjar et al. 2003) at orbital distances compared to the high eccentric exoplanets HD 108147b (Pepe et al. 2002) and HD 162020b (Udry et al. 2002) and the giant planet HD 28185b (Santos et al. 2001) at an orbital distance of ≈ 1.03 AU, and to predict qualitatively corresponding regimes of the stellar wind interaction with exoplanets. It should be noted that the host stars of OGLE-TR-56b, HD 209458b, and HD 28185b are solar-like stars with masses close to $\approx 1 M_{\rm Sun}$, while HD 108147 is a F8/G0 V-type star with $\approx 1.27 M_{\rm Sun}$ and HD 162020 is a K2 V star with a mass $\approx 0.7 M_{\rm Sun}$. With HD 209458b as a representative for short periodic hydrogen-rich gas giants, we use our modeled plasma parameters for the calculation of hydrogen ionization rates and estimations of planetary ion loss rates and discuss related plasma effects in the star-exoplanet environment.

2. STELLAR WIND PARAMETERS AND MACH NUMBERS IN THE PLASMA REGIME OF SHORT-PERIODIC AND ECCENTRIC EXOPLANETS

In order to analyze whether bow shocks will occur in front of short-periodic exoplanets owing to the interaction with the stellar wind, it is necessary to calculate the Alfvén Mach number $M_{\rm A}$,

$$M_{\rm A} = \frac{v_{\rm sw}}{v_{\rm A}} = \frac{v_{\rm sw}\sqrt{\mu_0 \rho}}{B}, \tag{1}$$

and the magnetosonic Mach number $M_{\rm s}$,

$$M_{\rm s} = M_{\rm A}\left(1 + \frac{\gamma\beta}{2}\right)^{-1/2}, \tag{2}$$

where $v_{\rm sw}$ and $v_{\rm A}$ are the stellar wind and Alfvén velocity, respectively, μ_0 is the magnetic permeability, γ is the adiabatic coefficient, ρ is the particle density, and B is the interplanetary magnetic field strength. The plasma parameter β is given as the ratio of the thermal to the magnetic pressure. The magnetic field and the particle density are scaled from present solar value at 1 AU of $B = 4$ nT and $n = 10$ cm^{-3} with a r^{-2} dependence to smaller orbits. For the radial variations of the electron plasma temperature T_e we use an approximation from Schwenn & Marsch (1991, p. 100), giving

$$T_e = T_0 r^{-\alpha}, \tag{3}$$

where $\alpha \approx 0.7$–0.8, and $T_0 = 10^5$ K is the electron plasma temperature at 1 AU. If we use $\alpha = 0.8$, the temperature at $r = 0.01$ AU is about 4×10^6 K. If we assume that the proton

TABLE 1

Parameters Used to Determine the Mach Numbers at the Orbits of OGLE-TR-56 b (0.023 AU), HD 209458 b (0.045 AU), and HD 28185 b (1.03 AU) for Conditions of a 4.6 Gyr Old Solar-like Star

Object	r (AU)	$v_{\rm sw}$ (km s^{-1})	n (m^{-3})	T_e (K)	$B(nT)$	$M_{\rm A}$	M_s
OGLE-TR-56b	0.023	400	1.9×10^{10}	2.05×10^6	7560	0.3	0.3
HD 209458b	0.045	400	4.9×10^9	1.19×10^6	1970	0.6	0.6
HD 28185b	1	400	10^7	10^5	4	14.5	8.6

temperature is $T_p \approx T_e/2$ (Sonett et al. 1971) as a rough estimation, we are in good agreement with the temperature of the solar corona.

The corresponding values for all parameters at the orbits of three exemplary exoplanets considered in our study can be found in Table 1. One can see that at the orbit of HD 28185b ($M \approx 5.7M_{\rm Jup}$) at $\approx$1.03 AU (Santos et al. 2001), the stellar wind parameters lead to the occurrence of a bow shock (i.e., $M_s > 1$), while the short-periodic exoplanets OGLE-TR-56b ($M \approx 1.45M_{\rm Jup}$) and HD 209458b ($M \approx 0.69M_{\rm Jup}$) at orbital distances of $\approx$0.023 and $\approx$0.045 AU are located in a stellar wind plasma regime where no bow shocks appear.

Figure 1 shows the Mach numbers for this scenario as a function of the radial distance in order to find the transition region between the two regimes. If we assume a magnetic field strength of $\approx 4 \times 10^4$ nT at 0.01 AU (corresponding to 4 nT at the orbit of HD 28185b at 1.03 AU), the transition region lies at $\approx$0.075 AU. Taking a nominal magnetic field of $\approx 10^5$ nT at 0.01 AU orbital distance (corresponding to 10 nT at the orbit of HD 28185b at 1.03 AU), the transition region is shifted to an orbital distance of $\approx$0.2 AU. This result suggests that more than 30 known exoplanets would establish no bow shocks. If we consider a denser stellar wind, the transition region is shifted to closer orbital distances, which is also the case if we assume a faster stellar wind.

Another important parameter is the corona temperature of the host star. In the previous cases we used a corona temperature of 2×10^6 K, but we can also consider smaller stellar corona temperatures, e.g., $\approx 10^6$ and $\approx 5 \times 10^5$ K. For these cases we use $T_0 = 2.53 \times 10^4$ K and $T_0 = 1.26 \times 10^4$ K in equation (3), respectively. One can see in Figure 2 that in the submagnetosonic region the temperature does not play a crucial role. For larger orbital distances, the higher temperatures give smaller magnetosonic Mach numbers. It can also be seen that the location of the transition region ($M_s \approx 1$) does not depend strongly on the temperature.

In the solar system, all planets except Pluto have a very small eccentricity ϵ of their orbits, but many exoplanets with rather large eccentricities are observed. The reasons for their eccentric orbits is not well understood until now, but most proposed mechanisms invoke gravitationally scattering (Weidenschilling & Marzari 1996) or perturbations of planets by other planets (Chiang 2003), perhaps in resonances, or by interaction with the protoplanetary disk (Goldreich & Sari 2003).

Because of their high orbital eccentricity, some exoplanets cross the transition region between both plasma interaction regimes during their orbit around their host stars. The eccentricity is given as $\epsilon = c/a$, where a is the semimajor axis and c gives the distance of the focus from the center of the elliptical orbit. In this case the transition region lies at an orbital distance of $\approx$0.08 AU. The most prominent close-in giant planet with a large eccentricity is HD 108147b, which has a mass $M \approx 0.4M_{\rm Jup}$, a semimajor axis of $a = 0.104$ AU and an eccentricity of $\epsilon = 0.498$ (Pepe et al. 2002). Therefore, the perihelion is at $\approx$0.155 AU and the aphelion is at $\approx$0.052 AU, meaning that this exoplanet exhibits a bow shock during $\approx$3/4 of its orbital period but has no bow shock during $\approx$1/4 of its orbit. Another

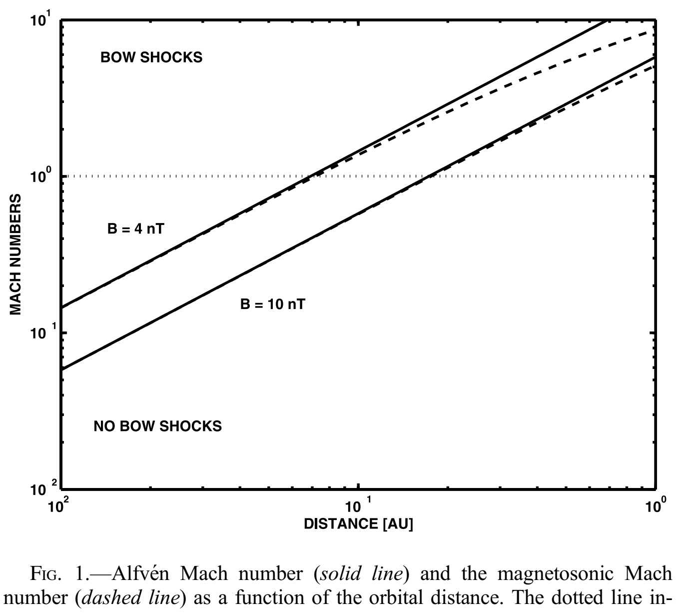

Fig. 1.—Alfvén Mach number (*solid line*) and the magnetosonic Mach number (*dashed line*) as a function of the orbital distance. The dotted line indicates the transition region. The Mach numbers are calculated for two magnetic field strengths (4 and 10 nT).

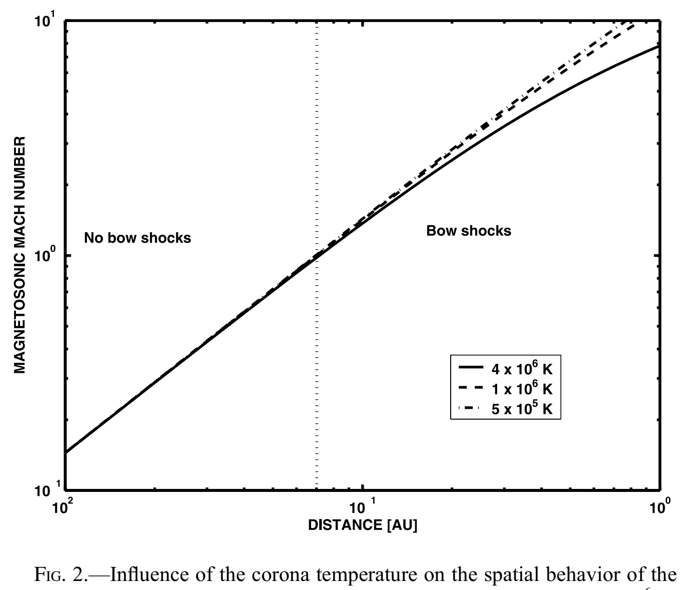

Fig. 2.—Influence of the corona temperature on the spatial behavior of the magnetosonic Mach number. For a stellar corona temperature of 4×10^6 K (*solid line*) smaller magnetosonic Mach numbers are achieved compared with lower temperatures of 10^6 K (*dashed line*) and 5×10^5 K (*dashed-dotted line*). The dotted line indicates the transition region between the submagnetosonic regime and the magnetosonic regime.

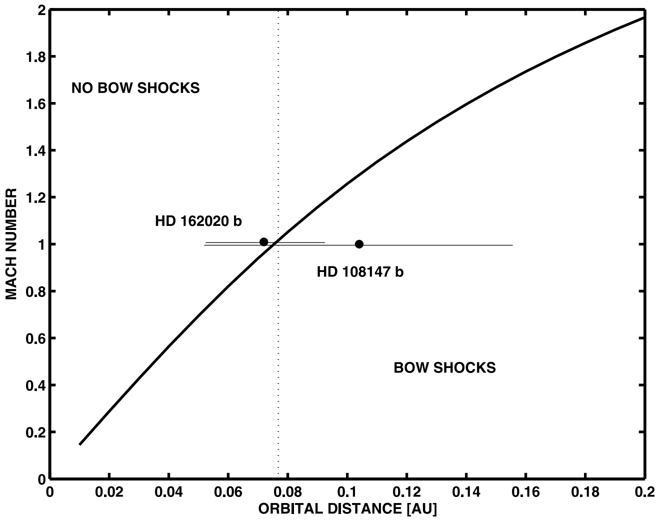

Fig. 3.—Eccentricity of the orbits of HD 108147b and HD 162020b and the magnetosonic Mach number. The dotted line separates the region where bow shocks occur from the region without bow shocks, while the thin solid lines indicate the eccentricity of the exoplanetary orbits.

candidate for crossing the transition region is HD 162020b with a mass $M \approx 13.75 M_{\rm Jup}$, a semimajor axis $a = 0.072$ AU and an eccentricity of $\epsilon = 0.277$ (Udry et al. 2002), which gives a perihelion distance of $\approx$0.092 AU and an aphelion distance of $\approx$0.052 AU.

More than half of its orbit, this exoplanet establishes no bow shock, but during the perihelion a bow shock appears. The orbital distance and the eccentricity of both exoplanets are shown in Figure 3. The properties of large Mach number regimes can be seen on examples of the solar wind interaction with the planets in the solar system. Our knowledge of this case is based on many observational data and results of theoretical calculations, especially for Earth, Venus, and Jupiter (Erkaev et al. 1998; Farrugia et al. 1998; Biernat et al. 2001). The main attributes of the large Mach number interaction is a shocked plasma flow in the magnetosheath including a relatively thin layer of enhanced magnetic field, which is called magnetic barrier. Magnetic forces are most important within this magnetic barrier.

The case of low Mach numbers is much less investigated on solar system bodies, however, some aspects of this case can also be analyzed owing to the similarity with the known cases of the magnetospheric plasma flow around large satellites in the Jupiter and Saturn systems. Effects regarding the change of plasma interaction regimes can be studied during the next years by the *Cassini* spacecraft because of the similarity of the interaction of Saturn's large satellite Titan with the ambient corotating magnetospheric plasma (Neubauer et al. 1984). A peculiarity of this case lies in the periodical variation of the external conditions for Titan: sometimes its orbit is inside Saturn's magnetosphere (low Mach number regime); at other times, the satellite can be outside the magnetosphere, where it is interacting directly with the solar wind plasma flow (large Mach number regime).

As pointed out before, for Mach numbers $M_s < 1$, the plasma interaction of the close-in gas giants does not lead to the formation of planetary bow shocks. Only Alfvén waves and slow shocks will be produced by this interaction regime. Assuming that these planets have very weak intrinsic magnetic moments owing to tidal locking (Grießmeier et al. 2004), the close distance to their host stars leads to a XUV-driven expanded upper atmosphere, giving rise to a Venus-like ionopause–stellar wind interaction (Lammer et al. 2003; Vidal-Madjar et al. 2003; Lecavelier des Etangs et al. 2004; Grießmeier et al. 2004). Therefore, we investigate in the following section the efficiency of various ionization processes and the resulting mass-loss rates of ionized particles from evaporating hydrogen-rich gas giants.

3. ION PRODUCTION AND PICK UP LOSS RATES AT GIANT EXOPLANETS AT SMALL ORBITAL DISTANCES

For the calculation of the ionized part of the evaporated neutral atmosphere, we take the well observed Jupiter-like exoplanet HD 209458b as a typical example for short-periodic gas giants in the slow shock regime at orbital distances less than 0.1 AU. It was proposed by Lecavelier des Etangs et al. (2004) that the exobase altitude of the expanded atmosphere of HD 209458b reaches the Roche lobe at a planetocentric distance of $\approx 3.6 R_{\rm Jup}$ so that the development of full energy-limited hydrodynamic "blow-off" conditions may not fully develop (Lecavelier des Etangs et al. 2004). Under this assumption and by using the vertical structure of the atmosphere as given by Lecavelier des Etangs et al. (2004) one can estimate the exobase number density n_c close to the Roche lobe from the exobase definition by the following relation (Bauer & Lammer 2004):

$$\int_{z_c}^{\infty} \frac{\mathrm{d}z}{\lambda(z)} = \int_{z_c}^{\infty} n(z)\sigma_c \, dz = n_c H \sigma_c \equiv \frac{H}{\lambda} = 1, \qquad (4)$$

where λ is the mean free path and σ_c is the collision cross section of $\approx 3 \times 10^{-15}$ cm^2. $H \approx 6.5 \times 10^4$ km is the scale height of atomic hydrogen. Because of exospheric temperatures in the order of about 10,000 K it is most likely that H_2 dissociated into H atoms (Coustenis et al. 1998). By using equation (4) we estimate an average exobase number density of about 5×10^4 cm^{-3} H atoms. Because, the estimation of the exobase number density in the so called "geometrical blow-off" regime of Lecavelier des Etangs et al. (2004) may contain uncertainties and should therefore, be considered as an average (mean) case, we model neutral gas profiles also for a minimal and maximal case with exobase number densities of about 1×10^4 cm^{-3} (min) and 1×10^5 cm^{-3} (max) H atoms, respectively. One should also note that the values of our exobase density estimation agree well with the observed Lyα absorption by Vidal-Madjar et al. (2003), which indicates that the hydrogen density at a planetocentric distance above the half Roche lobe of HD 209458b is in the order of about 2×10^5 cm^{-3}.

We simulate the neutral number density of the evaporating H atoms above the exobase by assuming a hot exobase with a temperature of 10,000 K (Lecavelier des Etangs et al. 2004) with the Monte Carlo model of Wurz & Lammer (2003). The neutral hydrogen atoms are directly released in the model from the exobase level with a most probable velocity corresponding to a temperature of 10,000 K. Our model follows the trajectory of each particle by numerical integration above the exobase until the particles reaches the end of the chosen calculation domain of $4R_{\rm pl}$. To studying the ionization processes and H^+ ion loss rates, we use a test particle model (Lichtenegger & Dubinin 1998; Lichtenegger et al. 2002), which was successfully used for the simulation of ion loss rates on Venus and Mars (Luhmann 1993; Lichtenegger et al. 1995; Lichtenegger & Dubinin 1998). The model involves the plasma parameters obtained by our calculations and shown in Table 1.

The total production rate of planetary H^+ ions is the sum of the rates of the main ionization processes, i.e., photoionization, electron impact ionization, and charge exchange. For the reaction of stellar wind protons with planetary H^+ ions, an energy-dependent charge exchange cross section σ_H has been employed (Kallio et al. 1997). The simulation of the particle fluxes is initialized by dividing the space around the planetary obstacle into a number of i volume elements ΔV. Production rates of planetary H^+ ions are then obtained by first calculating the absorption of the stellar wind flow along streamlines due to charge exchange with the evaporating atmospheric neutral gas. The stellar wind flux Φ_{sw} in an volume element ΔV_i at position $\boldsymbol{r}_i$ with respect to the planetary center is given by (Lichtenegger et al. 2002)

$$\Phi_{sw}(\boldsymbol{r}_i) = \Phi_{sw}^{(0)}(\boldsymbol{r}_i)e^{-\int_{\infty}^{s_i} n_H\sigma_H \, ds}, \tag{5}$$

where the integration is performed from the upstream stellar wind to the corresponding point s_i at position $\boldsymbol{r}_i$ on the streamline. $\Phi_{sw}^{(0)}$ is the unperturbed stellar wind flux, n_H the density of neutral H atoms as a function of altitude derived by using the model of Wurz & Lammer (2003), σ_H is the energy-dependent charge exchange cross section between a proton and the neutral H atom (Kallio et al. 1997), and ds is the line element along the streamline. The loss rates of stellar wind protons l_{sw} ($cm^{-3}\ s^{-1}$) due to the interaction with the evaporating atmospheric H atoms thus becomes $l_{sw}^H = \Phi_{sw}n_H\sigma_H$. The corresponding planetary H^+ ion production rates p due to charge exchange are assumed to be equal to the corresponding loss rates of the stellar wind, i.e., $p_H^{ce} = l_{sw}^H$. The rate of H^+ produced by electron impact is given by $p_H^{ei} = \nu_e n_e n_H$, where ν_e is the (temperature-dependent) ionization frequency per incident electron (Cravens et al. 1987) and n_e the electron density. The total planetary ion production rate of H atoms in each volume element is the sum

$$p_H^{tot} = p_H^{ei} + p_H^{ce} + p_H^{\gamma}, \tag{6}$$

with $p_H^{\gamma} = \nu_\gamma n_H$ being the rate due to photoionization, where ν_γ is the photon ionization frequency (Banks & Kockarts 1973).

Figure 4 shows the total ion production rates q_i for H^+ along a streamline caused by photoionization, electron impact and charge exchange with the stellar wind for the min (*solid lines*), average (*dashed lines*), and max (*dotted lines*) density profiles considered for HD 209458b at an orbital distance of 0.045 AU (slow shock regime: *three upper curves*) and for a similar planet at an orbital distance of 0.2 AU (fast shock regime: *three lower curves*). One can see that bow shocks develops in the fast shock regime at $\approx 3.5 R_{pl}$, while in the slow shock regime no jump in the ion production rate occurs. One can also see that the main ionization processes develop close to the planetary obstacle at $\approx 2.5 R_{pl}$ corresponding to $\approx 3.6 R_{Jup}$. It should be mentioned that in this model no mass-loading effects are included. Since the stellar wind particle density is much larger than the number of particles produced by the ionization effects mentioned above, we assume that the flow profiles are not influenced significantly by mass loading, and therefore this effect can be neglected in this estimation.

Our test particle simulations result in total H^+ ion loss rates for HD 209458b of $\approx 1.7\times 10^8$ g s^{-1} (min), $\approx 7.5\times 10^8$ g s^{-1} (mean), and $\approx 1.3\times 10^9$ g s^{-1} (max). One can see that our simulations give results, which are about factors 7–60 lower than previous H^+ loss estimations on Pegasi planets at similar orbital distances based on a simple scaling method by Guillot et al. (1996). Because the calculated ion loss rates are also lower than the observed and modeled neutral hydrogen winds our study indicates that the majority of the hydrogen that evaporates from hot gas giants escapes as neutral gas. Particle runs for a similar planet as HD 209458b in the fast shock region at an orbital distance of about 0.2 AU (see Fig. 2) give lower ion loss rates in the order of $\approx 10^7$ g s^{-1} (min), $\approx 5\times 10^7$ g s^{-1} (mean), and $\approx 8.3\times 10^7$ g s^{-1} (max).

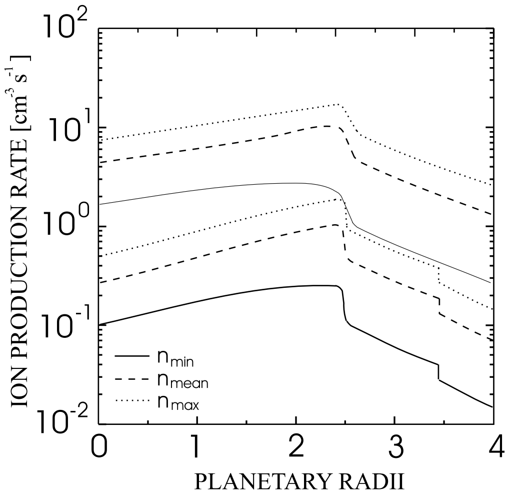

FIG. 4.—Total hydrogen ion production rates (charge exchange, XUV ionization, electron impact ionization) of the evaporating hydrogen atmosphere of HD 209458b at an orbital distance of 0.045 AU (slow shock regime: *three upper curves*) and a hypothetical similar exoplanet at 0.2 AU (fast shock regime: *three lower curves*) as a function of planetary radii. The solid curves correspond to an exobase H number density of 10^4 cm^{-3}, the dashed curves to 5×10^4 cm^{-3}, and the dotted lines to 10^5 cm^{-3}.

Nevertheless, our calculated ion loss rates in the order of about 10^8–10^9 g s^{-1} for gas giants with orbits inside the slow shock regime might be comparable to the Io-Jupiter plasma interaction, which takes into account a pressure disturbance in the vicinity of Io due to volcanic eruptions and ejection of planetary ions into Io-Jupiter flux tubes (Erkaev et al. 2001). The pressure pulse generates two slow mode waves propagating along the Io-Jupiter flux tube into the northern and southern hemisphere of Jupiter. These slow waves evolve rather quickly into nonlinear waves because of a steepening mechanism with a supersonic plasma flow just behind the shock (Langmayr et al. 2005). A consequence of the Io-Jupiter electrodynamic interaction are nonthermal radio emissions from the Io-Jupiter flux tube (Dessler 1983; Genova & Aubier 1985; Shaposhnikov et al. 2000). However, Zarka et al. (2001) argued that short-periodic Jupiter-class exoplanets around their star, analogous to the Io-Jupiter plasma interaction are unlikely to continuously produce intense radio emissions, unless the host star is very strongly magnetized.

On the other hand, a direct stellar wind interaction with the ionized part of the upper atmosphere may lead to an enhanced flow of planetary plasma in magnetic flux tubes, which connect the host star. The interaction with the stellar magnetosphere could then produce magnetic reconnection, and as a consequence, lead to accelerated ions, which may be responsible for chromospheric heating on the stellar surface (Ip et al. 2004; Rubenstein & Schäfer 2000; Cuntz et al. 2000; Cuntz & Shkolnik 2002). Rubenstein & Schäfer (2000) suggested that a magnetospheric interaction may even lead to superflares on the surface of solar-type stars, which would also have an impact on the exoplanet, where for example, particle heating and large auroras may be created (Ip et al. 2004).

4. CONCLUSIONS

Our results indicate that short-periodic giant exoplanets like OGLE-TR-56b and HD 209458b at orbital distances less than 0.1–0.2 AU around solar-like stars with ages comparable to our Sun orbit in a stellar wind plasma environment where no bow shocks evolve. In such a plasma interaction only slow shocks and Alfvén waves will develop. Hydrogen-rich gas giants experience XUV-driven atmospheric expansion and strong planetary neutral hydrogen winds. In comparison, we calculated ion production rates of evaporating H atoms and found ion loss rates for HD 209458b in the orders of about 10^8–10^9 g s^{-1}, which are lower than the observational based and modeled neutral hydrogen loss rates of about 10^{10}–10^{12} g s^{-1} (Vidal-Madjar et al. 2003; Lammer et al. 2003; Lecavelier des Etangs et al. 2004; Baraffe et al. 2004). This exoplanet–star plasma interaction may be comparable with the Io-Jupiter interaction, so that nonthermal radio bursts from exoplanet-stellar flux tubes may be created and magnetic reconnection may accelerate planetary ions to the host stars surface. Exoplanets with large eccentric orbits like HD 108147b and HD 162020b exhibit bow shocks and no shock periods during the movement around their host stars. For exoplanets in larger orbital distances, a super-magnetosonic stellar wind interaction takes place. This leads to changes in the flow profiles and also in the production rates. Future studies should investigate the role of both interaction regimes on full hydrodynamic energy-limited "blow-off" conditions and related effects like magnetic reconnection and the generation of plasma waves due to the star-magnetosphere-atmosphere interaction of close-in giant exoplanets. Additionally, the influence of mass loading on the plasma flow around the planetary obstacles of short-periodic gas giants should be studied in more details.

The authors wish to thank an anonymous referee for constructive suggestions, which helped to improve this paper. This work is supported by grants E02-8.0-22 from the Russian Ministry of Higher Education, by grants 04-05-64088, 03-05-20014_BNTS_a from the Russian Foundation of Basic Research, and by project Nr. I.2/04 from "Österreichischer Austauschdienst." It is also supported by the Austrian "Fonds zur Förderung der wissenschaftlichen Forschung" under project P17099-N08 and the Ministery for Education, Science and Culture (project Extractor). We acknowledge also the support by the Austrian Academy of Sciences, "Verwaltungstelle für Auslandsbeziehungen," the Russian Academy of Sciences, and the Austrian Ministry for Science, Education and Culture (bm:bwk) for supporting the CoRoT project.

REFERENCES

Arshukova, I. L., Erkaev, N. V., Biernat, H. K., & Vogl, D. F. 2004, Adv. Space Res., 33, 182
Banks, P. M., & Kockarts, G. 1973, Aeronomy, Part A (New York: Academic Press)
Baraffe, I., Selsis, F., Chabrier, G., Barman, T. S., Allard, F., Hauschildt, P. H., & Lammer, H. 2004, A&A, 419, L13
Bauer, S. J., & Lammer, H. 2004, Planetary Aeronomy: Atmosphere Environments in Planetary Systems (Heidelberg: Springer)
Biernat, H. K., Erkaev, N. V., & Farrugia, C. J. 2001, Adv. Space Res., 28, 833
Burrows, A., Hubeny, I., Hubbard, W., Sudarsky, D., & Fortney, J. 2004, ApJ, 610, L53
Chiang, E. I. 2003, ApJ, 584, 465
Coustenis, A., et al. 1998, ASP Conf. Ser. 134, Brown Dwarfs and Extrasolar Planets, ed. R. Rebolo et al. (San Francisco: ASP), 296
Cravens, T. E., Kozyra, J. U., Nagy, A. F., Gombosi, T. I., & Kurtz, M. 1987, J. Geophys. Res., 92, 7341
Cuntz, M., Saar, S. H., & Musielak, Z. E. 2000, ApJ, 533, L151
Cuntz, M., & Shkolnik, E. 2002, Astron. Nachr., 323, 387
Dessler, A. J., ed. 1983, Physics of the Jovian Magnetosphere (Cambridge: Cambridge Univ. Press)
Erkaev, N. V., Farrugia, C. J., & Biernat, H. K. 1998, J. Geophys. Res., 104, 6877
———. 2003, Planet. Space Sci., 51, 745
Erkaev, N. V., Semenov, V. S.,Shaidurov, V. A., Langmayr, D., Biernat, H. K., & Rucker, H. O. 2001, Adv. Space Res., 28, 1481
Farrugia, C. J., Biernat, H. K., & Erkaev, N. V. 1998, Planet. Space Sci., 46, 507
Genova, F., & Aubier, M. G. 1985, A&A, 150, 139
Goldreich, P., & Sari, R. 2003, ApJ, 585, 1024
Grießmeier, J.-M., et al. 2004, A&A, 425, 753
Guillot, T., Burrows, A., Hubbard, W. B., Lunine, J. I., & Saumon, D. 1996, ApJ, 459, L35
Ip, W.-H., Kopp, A., & Hu, J.-H. 2004, ApJ, 602, L53
Kallio, E., Luhmann, J. G., & Barabash, S. 1997, J. Geophys. Res., 102, 22183
Konacki, M., Torres, G., Jha, S., & Sasselov, D. 2003, Nature, 421, 507
Lammer, H., Selsis, F., Ribas, I., Guinan, E. F., Bauer, S. J., & Weiss, W. W. 2003, ApJ, 598, L121
Langmayr, D., Shaidurov, V. A., Erkaev, N. V., Biernat, H. K., & Rucker, H. O. 2005, Recent Res. Develop. Plasmas, in press
Lecavelier des Etangs, A., Vidal-Madjar, A., McConnell, J. C., & Hébrard, G. 2004, A&A, 418, L1
Lichtenegger, H. I. M., & Dubinin, E. M. 1998, Earth Planet. Space, 50, 445
Lichtenegger, H. I. M., Lammer, H., & Stumptner, W. 2002, J. Geophys. Res., 107, 1279
Lichtenegger, H. I. M., Schwingenschuh, K., Dubinin, E. M., & Lundin, R. 1995, J. Geophys. Res., 100, 21659
Luhmann, J. G. 1993, J. Geophys. Res., 98, 17615
Moutou, C., et al. 2003, in ASP Conf. Ser. 294, Scientific Frontiers on Extrasolar Planets, ed. D. Deming & S. Seager (San Francisco: ASP), 423
Neubauer, F. M., Gurnett, D. A., Scudder, J. D., & Hartle, R. E. 1984, in Saturn, ed. T. Gehrels, & M. S. Matthews (Tucson: Univ. Arizona Press), 760
Penz, T., Lammer, H., Erkaev, N. V., Grießmeier, J.-M., Vogl, D. F., Biernat, H. K., Hanslmeier, A., & Weiss, W. W. 2004a, in Proc. Phys. of Auroral Phenomena (Apatity: Polar Geophys. Inst.), 39
Penz, T., et al. 2004b, Planet. Space Sci., 52, 1157
Pepe, F., Mayor, M., Galland, F., Naef, D., Queloz, D., Santos, N. C., Udry, S., & Burnet, M. 2002, A&A, 388, 632
Rubenstein, E. P., & Schäfer, B. E. 2000, ApJ, 529, 1031
Santos, N. C., Mayor, M., Naef, D., Pepe, F., Queloz, D., Udry, S., & Burnet, M. 2001, A&A, 379, 999
Schwenn, R., & Marsch, E. 1991, Physics of the Inner Heliosphere II (Berlin: Springer)
Shaposhnikov, V. E., Rucker, H. O., & Zaitsev, V. V. 2000, A&A, 355, 804
Sonett, C. P., Coleman, P. J., & Wilcox, J. M., eds. 1971, Solar Wind (Pacific Grove: NASA)
Udry, S., Mayor, M., Pepe, F. Queloz, D., Santos, N., & Burnet, M. 2002, A&A, 390, 267
Vidal-Madjar, A., Lecavelier des Etangs, A., Désert, J.-M., Ballester, G. E., Ferlet, R., Hébrard, G., & Mayor, M. 2003, Nature, 422, 143
Vidal-Madjar, A., et al. 2004, ApJ, 604, L69
Watson, A. J., Donahue, T. M., & Walker, J. C. G. 1981, Icarus, 48, 150
Weidenschilling, S. J., & Marzari, F. 1996, Nature, 384, 619
Wurz, P., & Lammer, H. 2003, Icarus, 164, 1
Yelle, R. 2004, Icarus, 170, 167
Zarka, P., Treumann, R. A., Ryabov, B. P., & Ryabov, V. B. 2001, Ap&SS, 277, 293